Volume 24, No 4 | International Journal of Radiation Research, October 2026

Plan quality analysis of intracranial stereotactic radiosurgery treatment planning in different grid sizes and photon fluence smoothness

A. Watcharawipha[1,2], W. Nobnop[1,2], A. Bunnachak[1], A. Chaiyapong[1], B. Jia-Mahasap[1], I. Chitapanarux[1,2]

[1]*Division of Radiation Oncology, Department of Radiology, Faculty of Medicine, Chiang Mai University, Chiang Mai, Thailand*

[2]*Medical Physics Program, Department of Radiology, Faculty of Medicine, Chiang Mai University, Chiang Mai, Thailand*

► ***Original article***

Corresponding author:
Wannapha Nobnop, Ph.D.,
E-mail: *wannapha.n@cmu.ac.th*

Received: April 2025
Final revised: April 2026
Accepted: April 2026

Int. J. Radiat. Res., October 2026; 24(4): 1031-1037

DOI: 10.61186/ijrr.24.4.13

Keywords: *Stereotactic radiosurgery, dose calculation, dose optimization, photon fluence smoothness, treatment planning.*

ABSTRACT

Background: Inverse treatment planning provides superior dose conformity and steep dose gradients, which are essential for Stereotactic Radiosurgery and Radiotherapy (SRS/SRT). Given the critical nature of dose optimization and calculation, this study investigates how different grid sizes and photon fluence smoothing levels influence plan quality outcomes. ***Materials and Methods:*** Using ten SRS/SRT cases, eight distinct planning scenarios were generated by cross-referencing 2 mm and 3 mm grid sizes for both optimization and final dose calculation, alongside two levels of fluence smoothing. Plan quality was evaluated via dose coverage, Homogeneity Index (HI), Conformity Index (CI), and Gradient Distance (GD). Statistical significance was assessed at a 95% confidence interval, utilizing a weighted scoring system to benchmark performance against a standard 2 mm grid protocol. ***Results:*** Utilizing a 3 mm grid for optimization followed by a 2 mm grid for final dose calculation yielded significantly better results for dose coverage and GD, though it produced a lower CI. Despite this, the weighted performance scores for this configuration exceeded the benchmark. Furthermore, the level of photon fluence smoothing (low vs. medium) did not significantly impact the plan quality outcome. ***Conclusion:*** A larger optimization grid (3 mm) paired with a finer calculation grid (2 mm) produces plan quality comparable to using a fine grid for both stages. These results suggest that planning efficiency can be improved without compromising clinical quality, regardless of the fluence smoothing level.

INTRODUCTION

Stereotactic radiosurgery and radiotherapy (SRS/SRT) are characterized by the delivery of high radiation doses over a limited number of treatment sessions. Originally developed for intracranial lesions, this technique is now implemented across various platforms, including Gamma Knife® [1, 2], Linear accelerators (Linacs) [1, 3], Tomotherapy [4-7], and CyberKnife® [7-8]. In Linac-based treatments, beam shaping is typically achieved using either Cylindrical Collimators (CC) or Multi-Leaf Collimators (MLC). While CCs are often preferred for their superior plan quality in treating small [3, 9], solitary lesions, MLCs remain a versatile alternative [3, 9-11]. They facilitate advanced delivery methods such as 3D conformal radiotherapy (3DCRT), intensity-modulated radiotherapy (IMRT), and intensity-modulated arc therapy (IMAT).

IMAT is frequently utilized in SRS/SRT because it merges intensity modulation with rotational arc delivery. This complex approach necessitates sophisticated treatment planning to optimize photon fluence, ensuring a balance between target coverage and the protection of Organs at Risk (OARs). The precision of these calculations is heavily influenced by the selected grid size within the Treatment Planning System [12, 13] (TPS). While finer grid sizes enhance accuracy, they often extend planning time and can introduce noise into dose distributions [13]. Consequently, planner must choose appropriate grid sizes for both the optimization and final dose calculation stages.

During optimization, the TPS determines the photon fluence for the target and surrounding OARs. This process includes a "photon fluence smoothness" setting, which manages the transition of fluence between adjacent voxels in the optimization grid. Together, the optimization grid, dose calculation grid, and smoothness settings significantly influence the final plan quality, especially for small lesions [14, 15]. While high-volume cancer centers must balance accuracy with efficiency, the specific interaction between these three parameters remains under-

[Downloaded from mail.ijrr.com on 2026-11-11]

[DOI: 10.61186/ijrr.24.4.13]

researched. Although previous studies have examined the impact of dose calculation grid sizes [12-15], there is a lack of data regarding how they interplay with optimization grids and fluence smoothing. This study aims to fill that gap by evaluating these relationships within the context of intracranial SRS/SRT.

MATERIALS AND METHODS

Ethical statement

Treatment planning information was retrospectively compiled from patients undergoing intracranial SRS/SRT from early 2022 through April 2023. This research was conducted in accordance with the approval of the Faculty of Medicine Research Ethics Committee, Chiang Mai University (Study code: RAD-2566-0157).

Computed tomography simulation image set

Eligible patients for SRS/SRT underwent immobilization via a bi-valve stereotactic thermoplastic mask system (Models R406-1 and RBSRS-02, Klarity®, Guangzhou, China,), which integrated a bite-block for stability. For treatment planning, a 1mm-slice CT scan was captured using a SOMATOM® Definition AS simulator (Siemens Healthineer Inc., Forchheim, Germany). To ensure precise delineation of the target volumes and organs at risk (OARs), these CT images were co-registered with 3D T1-weighted MR images (1mm thickness) obtained from a 1.5T SIGNA Horizon scanner (GE Healthcare, WI, USA). The Planning Target Volume (PTV) was defined by applying a 2 mm margin to the Gross Tumor Volume (GTV). Patient demographics are summarized in table 1.

Table 1. Patient characteristics and beam geometries of the intra-cranial SRS/SRT.

Case	Dx	GTV (cc)	PTV (cc)	Prescription (Gy)	Fxs	Arc (No.)	Arc range (degree)	Couch angle (degree)
1	AVM	0.11	0.26	20.0	1	5	300/ 300/130/ 130/ 130	0/ 0/270/ 315/ 45
2	Vestibular schwannoma	0.14	0.54	25.0	5	4	300/130/ 130/ 130	0/270/ 315/ 45
3	Brain metastasis	0.68	1.21	20.0	1	5	300/ 300/130/ 130/ 130	0/ 0/270/ 315/ 45
4	DAVF	1.03	1.91	20.0	1	5	300/ 300/130/ 130/ 130	0/ 0/270/ 315/ 45
5	Pituitary macroadenoma	1.34	2.23	25.0	5	4	300/ 130/ 130/ 130	0/ 270/ 315/ 45
6	AVM	1.99	4.75	28.0	4	4	300/ 130/ 130/ 130	0/ 270/ 315/ 45
7	AVM	2.67	6.23	28.0	4	4	300/130/ 130/ 130	0/270/ 315/ 45
8	Brain metastasis	5.97	17.23	27.0	3	4	300/130/ 130/ 130	0/270/ 315/ 45
9	AVM	10.78	20.89	28.0	4	4	300/130/ 130/ 130	0/270/ 315/ 45
10	AVM	15.75	25.76	30.0	5	4	300/130/ 130/ 130	0/270/ 315/ 45
Mean		4.05	8.10	25.10	3.3	4.3		
SD		5.28	9.50	3.81	1.7	0.5		
Median		1.67	3.49	26.00	4.0	4.0		
Min		0.11	0.26	20.00	1.0	4.0		
Max		15.75	25.76	30.00	5.0	5.0		

Abbreviations: Dx; Diagnosis, GTV; Gross target volume, PTV; Planning target volume, Fxs; Fractions, cc; Cubic centimeter, Gy; Gray, No.; Number, AVM; Arteriovenous malformation, DAVF; Dural arteriovenous fistula, SD; Standard deviation, Min; Minimum and Max; Maximum.

Treatment planning scenarios

Between January 2022 and April 2023, ten treatment plans for patients with single intracranial lesions were retrospectively selected for analysis. All plans utilized Volumetric Modulated Arc Therapy (VMAT) delivered via a 6 MV C-arm linear accelerator (Synergy®, Elekta Inc., Crawley, UK). The specific beam geometries, dose prescriptions, and fractionation schedules employed in clinical practice are summarized in table 1. The treatment planning process was conducted using the Monaco® TPS (Version 5.11, Elekta Inc., MO, USA), utilizing the Monte Carlo algorithm for dose distribution. While standard clinical protocol employed a 2 mm grid size for both optimization and final dose calculation - along with a random selection of either "Medium" or "Low" photon fluence smoothness - this study expanded those parameters. Specifically, eight distinct scenarios were evaluated by varying the photon fluence smoothness levels and the grid sizes for optimization (O) and calculation (C). These scenarios, labeled as O/Cmm, are illustrated in figure 1. To ensure plan quality, the following target constraints were strictly applied; *Coverage:* At least 99% of the Planning Target Volume (PTV) was required to receive the full prescription dose. *Maximum dose* (D_{max}): The highest dose was limited to less than 125% of the prescribed dose.

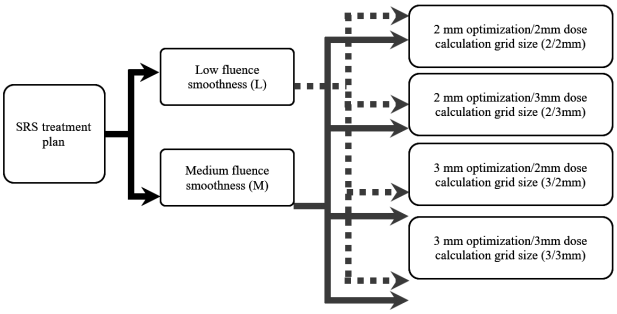


Figure 1. Schematic treatment planning by utilizing various values of the plan parameters. SRS treatment plan was replanned using different photon fluence smoothness. Each of this plan was conducted in an interplay between optimization and dose calculation grid size.

Evaluation of treatment plans

Plan quality was assessed by analyzing target coverage, maximum dose (D_{max}) and minimum dose

[Downloaded from mail.ijrr.com on 2026-11-11]

[DOI: 10.61186/ijrr.24.4.13]

(D_{min}) thresholds for the target volume, and D_{max} of OARs, including the brainstem, optic chiasm, optic nerves, globes, lenses, and cochleae. Peripheral dose distribution was also monitored, specifically examining the volume of the brain and external contour receiving a dose at 12 Gy. Furthermore, PTV analysis incorporated several established metrics: the Homogeneity Index [5, 16, 17] (HI), Conformity Index [18] (CI), Conformity Index at 50% of the prescribed isodose [5,17,19-20] (CI_{50}), and Gradient Distance [5, 17, 21, 22] (GD).

Homogeneity Index (HI): This metric evaluates the uniformity of the dose distribution within the target area. It is determined by the ratio of the maximum dose to the prescribed dose (D_{max}/D_{Rx}).

Conformity Index (CI): To assess how well the prescription dose encompasses the target, the Paddick formalism [18] was employed, which is particularly suited for SRS/SRT applications. It is calculated as: $TV^2_{PIV}/(PTV \times PIV)$ where PTV is the Planning Target Volume, PIV is the volume encompassed by the prescription isodose, and TV_{PIV} is the volume of the target receiving the prescription dose.

Conformity Index at 50% (CI_{50}): This index characterizes the spread of low-level radiation surrounding the target. It is defined as the ratio of the volume receiving 50% of the prescribed dose (PIV_{50}) to the: PIV_{50}/PIV.

Gradient Distance (GD): While CI_{50} offers a ratio, the GD provides a linear measurement (in cm or mm) of the dose fall-off. Adapted from the Conformity Gradient Index (CGI) for greater clarity, it calculates the distance between the equivalent radii of the 50% and 100% isodose volumes: ($\sqrt[3]{3PIV_{50}/4\pi}$-$\sqrt[3]{3PIV/4\pi}$).

Statistical evaluation and treatment plan performance

To evaluate the performance of the eight treatment planning scenarios against the high-resolution benchmark, a comprehensive statistical analysis was conducted. Data normality was first assessed using the Shapiro-Wilk test. Based on these results, a Paired Student's *t*-test was applied to normally distributed datasets, while the Wilcoxon Signed-Rank Test was utilized for non-parametric data. All statistical computations were performed using SPSS version 25 (IBM Co., NY, USA). Results were considered statistically significant at a 95% confidence interval ($p<0.05$). Furthermore, the performance scores for each scenario were weighted relative to their respective smoothness benchmarks [23]. To determine the impact of resolution across different photon smoothness categories, the finest resolution within the low-smoothness tier was compared directly against the medium-smoothness tier.

RESULTS

Table 2 summarizes the dosimetric outcomes for the target volume across eight distinct scenarios, while table 3 details the corresponding results for the OARs. To identify significant variations, a statistical analysis was performed to evaluate the impact of optimization and dose calculation grid sizes, as well as photon smoothing levels. These comparisons were conducted across all planned scenarios, utilizing the 2/2mm grid configuration as the established benchmark for performance.

Different dose calculation grid size comparison

When the optimization grid sizes were kept consistent across plan scenarios, notable variations in dosimetry parameters emerged, with statistical significance ($p<0.05$) highlighted by the asterisk (*) symbol. For target dosimetry at a low photon smoothness level, the 2 mm calculation grid size yielded significantly better results for target coverage ($p \leq 0.009$), D_{min} ($p \leq 0.028$), and GD ($p=0.004$), though it produced significant inferior CI values ($p=0.005$) regardless of the optimization grid size used. Within the specific 2 mm optimization grid cohort, the 2 mm calculation grid showed significant superior CI_{50} ($p = 0.007$) but resulted in significantly poorer D_{max} ($p=0.005$) and HI ($p=0.007$) outcomes. Similar trends were noted at the medium photon smoothness level, where the 2 mm calculation grid remained significant superior for target coverage ($p \leq 0.007$), D_{min} (p £ 0.011), and GD ($p=0.005$), while D_{max} (p£0.013), HI ($p=0.011$) and CI ($p \leq 0.007$) were consistently significant inferior across both optimization settings. Additionally, the CI_{50} ($p=0.005$) for the 2 mm optimization grid outperformed the 3 mm calculation grid, whereas no significant dosimetric differences were detected regarding OARs across any of the tested treatment scenarios.

Different optimization grid size comparison

When dose calculation grid sizes were kept consistent across treatment plans, several significant dosimetric variations (marked by †) emerged between different optimization grid settings. Specifically, at a low photon fluence smoothness level, employing a 2 mm optimization grid produced a significantly better CI ($p=0.005$) compared to a 3 mm grid, yet it yielded inferior results for target coverage ($p \leq 0.009$) and GD ($p \leq 0.011$) regardless of the final calculation grid size. Within the 3 mm calculation grid cohort, the 2 mm optimization setting provided significant superior outcomes for D_{max} ($p=0.022$) and HI ($p=0.016$). Under medium smoothness conditions, the 2 mm optimization grid continued to show significantly better D_{max} ($p \leq 0.013$), HI ($p \leq 0.012$), and CI ($p=0.007$) values, while

[Downloaded from mail.ijrr.com on 2026-11-11]

[DOI: 10.61186/ijrr.24.4.13]

consistently significant underperforming in target coverage (p≤0.017) and GD (p≤0.016) across both calculation scales. Notably, the 2 mm calculation grid only showed a significant improvement in CI_{50} (p=0.037) when paired with 2 mm optimization. Finally, no significant discrepancies were detected in the sparing of OARs across the various planning scenarios.

Table 2. Mean value and standard deviation (Mean ± SD) of dosimetric parameters on the target using different dose optimization grid sizes, dose calculation grid size, and photon fluence smoothness level, and weighted score of each plan scenario.

Fluence		**Low photon smoothness**				**Medium photon smoothness**			
Grid (Opt./D_{cal})	mm	2/2	2/3	3/2	3/3	2/2	2/3	3/2	3/3
Coverage	%	99.29 ± 0.38	97.48 ± 1.07	99.63 ± 0.27	99.24 ± 0.20	99.32 ± 0.39	96.61 ± 2.17	99.65 ± 0.26	99.20 ± 0.23
		*(p = 0.009) †(p = 0.017)	†(p = 0.007) ‡(p = 0.009)	*(p = 0.005) ‡(p = 0.017)		*(p = 0.007) †(p = 0.017)	†(p = 0.005) ‡(p = 0.007)	*(p = 0.005) ‡(p = 0.017)	
score		0	-1	1	0	0	-1	1	0
D_{min}	Gy	24.20 ± 3.61	23.72 ± 3.67	24.24 ± 3.28	23.95 ± 3.20	24.31 ± 3.52	23.69 ± 3.55	24.13 ± 3.23	23.77 ± 3.17
		*(p = 0.005)	‡(p = 0.005)	*(p = 0.028)		*(p = 0.005)	‡(p = 0.005)	*(p = 0.011)	‡(p = 0.022)
score		0	-1	0	0	0	-1	0	-1
D_{max}	Gy	30.70 ± 4.55	30.06 ± 4.49	31.46 ± 4.50	31.28 ± 4.89	30.87 ± 4.67	30.35 ± 4.80	31.73 ± 4.79	31.32 ± 4.85
		*(p = 0.005)	†(p = 0.022) ‡(p = 0.005)			*(p = 0.013) †(p = 0.013)	†(p = 0.009) ‡(p = 0.013)	*(p = 0.005) ‡(p = 0.013)	‡(p = 0.037)
score		0	1	0	0	0	1	-1	-1
HI	-	1.22 ± 0.02	1.20 ± 0.02	1.26 ± 0.07	1.25 ± 0.03	1.23 ± 0.02	1.21 ± 0.02	1.26 ± 0.03	1.25 ± 0.03
		*(p = 0.007)	†(p = 0.016) ‡(p = 0.007)			*(p = 0.011) †(p = 0.012)	†(p = 0.008) ‡(p = 0.011)	*(p = 0.011) ‡(p = 0.012)	‡(p = 0.045)
score		0	1	0	0	0	1	-1	-1
CI	-	0.74 ± 0.08	0.78 ± 0.06	0.64 ± 0.11	0.68 ± 0.11	0.75 ± 0.07	0.79 ± 0.05	0.64 ± 0.10	0.68 ± 0.10
		*(p = 0.005) †(p = 0.009)	†(p = 0.011) ‡(p = 0.005)	*(p = 0.005) ‡(p = 0.009)	‡(p = 0.041)	*(p = 0.007) †(p = 0.007)	†(p = 0.007) ‡(p = 0.007)	*(p = 0.005) ‡(p = 0.007)	‡(p = 0.022)
score		0	1	-1	-1	0	1	-1	-1
CI_{50}	-	7.22 ± 4.29	7.53 ± 4.48	7.20 ± 4.01	7.25 ± 3.96	6.76 ± 3.79	7.17 ± 3.91	7.17 ± 3.80	7.21 ± 3.79
		*(p = 0.007)	‡(p = 0.007)			*(p = 0.005) †(p = 0.037)	‡(p = 0.005)	‡(p = 0.037)	‡(p = 0.037)
score		0	-1	1	0	0	-1	-1	-1
GD	mm	6.83 ± 1.62	7.14 ± 1.58	6.32 ± 1.38	6.58 ± 1.37	6.66 ± 1.65	6.97 ± 1.61	6.37 ± 1.44	6.60 ± 1.45
		*(p = 0.004) †(p = 0.011)	†(p = 0.008) ‡(p = 0.004)	*(p = 0.004) ‡(p = 0.011)		*(p = 0.005) †(p = 0.016)	†(p = 0.007) ‡(p = 0.005)	*(p = 0.005) ‡(p = 0.016)	
score		0	-1	1	0	0	-1	1	0
Sum score		0	-1	**1**	-1	0	-1	-2	-5

Significant difference: *; Optimization grid size/2 vs Optimization grid size /3, †; 2/Calculation grid size vs 3/Calculation grid size and ‡; each plan scenario vs 2/2 benchmark. **Abbreviations:** Grid (Opt/Dcal); Optimization grid size/Dose calculation grid size, D_{min}; Minimum dose, D_{max}; Maximum dose, HI; Homogeneity index, CI; Conformity index, CI_{50}; Conformity index at 50% dose prescription, and GD; Gradient distance.

Table 3. Mean Value and Standard Deviation (Mean ± SD) of Dosimetric Parameters on the Organs at Risk Using Different Dose Optimization Grid Sizes, Dose Calculation Grid Size, and Photon Fluence Smoothness level.

Fluence		**Low photon smoothness**				**Medium photon smoothness**			
Grid (Opt/D_{cal})	mm	2/2	2/3	3/2	3/3	2/2	2/3	3/2	3/3
Brainstem	Gy	7.59 ± 9.51	7.54 ± 9.48	7.93 ± 10.00	7.93 ± 10.02	7.89 ± 9.58	7.82 ± 9.57	8.09 ± 9.85	8.10 ± 9.84
Optic chiasm	Gy	4.26 ± 7.41	4.18 ± 7.49	4.50 ± 8.10	4.41 ± 7.93	4.61 ± 7.72	4.53 ± 7.48	4.67 ± 8.12	4.57 ± 8.00
Lt.Optic Nerve	Gy	3.55 ± 7.07	3.41 ± 6.85	3.54 ± 6.58	3.51 ± 6.61	3.80 ± 7.10	3.80 ± 7.14	3.52 ± 6.58	3.45 ± 6.48
Rt.Optic Nerve	Gy	1.83 ± 2.74	1.80 ± 2.77	1.63 ± 3.26	1.63 ± 3.26	1.96 ± 3.24	1.90 ± 3.17	1.68 ± 2.64	1.68 ± 2.66
Lt.Globe	Gy	1.21 ± 1.21	1.16 ± 1.15	1.43 ± 1.38	1.42 ± 1.39	1.31 ± 1.70	1.26 ± 1.63	1.54 ± 1.65	1.51 ± 1.63
Rt.Globe	Gy	1.57 ± 1.84	1.53 ± 1.83	1.67 ± 2.33	1.62 ± 2.25	1.89 ± 2.45	1.82 ± 2.34	1.65 ± 1.92	1.57 ± 1.80
Lt.Len	Gy	0.58 ± 0.76	0.57 ± 0.79	0.71 ± 1.02	0.69 ± 0.95	0.76 ± 1.18	0.75 ±1.18	0.84 ±1.30	0.81 ± 1.24
Rt.Len	Gy	0.82 ± 1.12	0.80 ± 1.09	0.86 ± 1.39	0.87 ± 1.40	1.02 ± 1.46	0.99 ± 1.42	0.63 ± 0.78	0.68 ± 0.70
Lt.Cochlea	Gy	2.23 ± 4.55	2.24 ± 4.58	2.46 ± 5.04	2.46 ± 5.06	2.43 ± 5.05	2.39 ± 4.98	2.56 ± 5.52	2.57 ± 5.56
Rt.Cochlea	Gy	3.68 ± 8.37	3.75 ± 8.48	3.51 ± 9.24	3.42 ± 8.95	3.56 ± 8.48	3.57 ± 8.44	3.66 ± 8.87	3.66 ± 8.90
Brain 12 Gy	cc	27.66 ± 33.55	27.72 ± 33.63	27.27 ± 31.68	27.38 ± 31.76	27.39 ± 34.10	27.57 ± 34.40	27.67 ± 31.93	27.78 ± 31.99
Dose volume 12 Gy	cc	43.20 ± 51.80	43.23 ± 52.01	42.43 ± 48.62	42.58 ± 48.67	42.85 ± 53.27	43.14 ± 53.77	43.24 ± 49.90	43.38 ± 49.97

Abbreviations: Grid (Opt/Dcal); Optimization grid size/Dose calculation grid size, Rt; Right, Lt; Left.

Different photon fluence smoothness level comparison

Within the same dose optimization and calculation grid parameters, the TPS utilizes various photon fluence smoothness levels to maintain dose consistency across adjacent voxels. Investigations into these settings revealed that transitioning from a low to a medium smoothness level yields no statistically significant impact on the resulting dose distribution, provided the grid size remains constant.

[Downloaded from mail.ijrr.com on 2026-11-11]

[DOI: 10.61186/ijrr.24.4.13]

Different plan scenario compared to the 2/2mm grid size benchmark and plan quality weighted score

To achieve high-precision treatment planning, a grid size of 2/2mm was established as the baseline for dose optimization and calculation. When compared to this standard across various photon fluence smoothness levels, other grid configurations exhibited significant dosimetric shifts (marked by ‡). Specifically, at the low smoothness level, the 2/3mm grid significantly improved D_{max} (p=0.005), HI (p=0.007) and CI (p=0.005), yet compromised target coverage (p=0.009), D_{min} (p=0.005), CI_{50} (p=0.007) and GD (p = 0.004). Conversely, the 3/2mm grid at this level significantly enhanced target coverage (p=0.017) and GD (0.011) but significantly degraded the CI (p=0.009), while the 3/3mm grid showed a significant decline only in CI (p=0.041). Within the medium smoothness level, the 2/3mm grid maintained its pattern of D_{max} (p=0.013), HI (p=0.011) and CI (p=0.007) alongside inferior target coverage (p=0.007), D_{min} (p=0.005), CI_{50} (p=0.005) and GD (p=0.005). The 3/2mm configuration under medium smoothness improved target coverage (p = 0.017) and GD (p=0.016) but negatively impacted D_{max} (p=0.013), HI (p=0.012), CI (p=0.007), and CI_{50} (p=0.037). Ultimately, the 3/3mm grid at medium smoothness yielded significantly inferior results across nearly all metrics, including D_{min} (p=0.022), D_{max} (p=0.037), HI (p=0.045), CI (p=0.022), and CI_{50} (p=0.037).

Determining the superior treatment plan proved challenging when comparing the various scenarios. However, using a 2/2mm grid size as the benchmark for weighted scoring highlighted significant disparities in dosimetry parameters. The analysis demonstrated that the 3/2mm grid size was the only configuration to achieve a positive score, while all other evaluated plans resulted in scores below zero.

DISCUSSION

The impact of grid size on treatment planning quality remains a critical area of investigation, specifically concerning the interplay between dose calculation, optimization grid sizes, and photon fluence smoothness. While previous literature has primarily focused on the dose calculation grid [13-15, 24-27], this study highlights that optimization grid size- which dictates photon fluence per unit volume - fundamentally influences the final dose calculation [25].

Extensive research has highlighted the critical role of dose calculation grid size in radiotherapy planning [13-15, 24-27]. Consistent with existing literature, this study observed that finer grid sizes improved target coverage and D_{min}, though plan quality indices such as the HI and CI appeared to decrease [24, 25], mirroring findings by Tongta *et al.* [25] These fluctuations stem from the direct impact of grid resolution on organ volume representation during dose optimization and calculation, particularly at target boundaries. As shown in figure 2, increasing the dose calculation grid size from 2 mm to 3 mm led to an artificial expansion of the 50% and 25% isodose volumes. This volumetric enlargement occurred consistently when transitioning from the 2 mm resolution (figures 2a, 2b, 2e, and 2f) to the 3 mm resolution (figures 2c, 2d, and 2h). Consequently, the impact on the CI was found to diminish as the dose calculation volume decreased. While our finding diverged from some studies [13, 15, 25] due to differences in indexing formulas, they align with the Conformation Number (CN) trends reported by Kim *et al.* [15] Consistent with the CI results, the HI followed a parallel trend; specifically, dose optimization grid size analysis revealed that plan quality improvements were more pronounced at medium photon smoothness levels compared to low levels. However, these CI and HI findings contrast with the results reported by Tongta *et al.* [25] This discrepancy is further evidenced by the distinct dose distributions observed between figures 2a–d and 2e–h, a variation that may be attributed to the utilization of different indexing formulas. Regarding the comparative analysis of photon fluence smoothness, no significant differences were observed between low and medium levels, suggesting this parameter may not be a critical determinant of overall plan quality. However, the impact of alternative smoothness levels warrants further investigation. While the study recommends utilizing the smallest possible grid size for optimal treatment plan construction, it acknowledges that this may increase preparation time- a practical concern for high-volume cancer centers managing heavy patient loads [26, 27] While this study did not evaluate treatment preparation duration, prior research by Tongta *et al.* [25] demonstrated that increasing grid size effectively reduces preparation time. Regarding doses to OARs, our findings showed no significant differences across normal tissues, which deviates from results reported in other studies [13, 15, 25] This discrepancy likely stems from variations in treatment techniques; specifically, SRS utilized here prioritized a steep dose gradient outside the target. Because the brain targets were localized, the impact on distant surrounding organs was minimized. Nevertheless, these results suggest that further investigation is warranted for targets located in immediate proximity to critical structures.

CONCLUSION

This study examined how the interplay between dose optimization grid size, dose calculation grid size, and photon fluence smoothness levels affects plan

[Downloaded from mail.ijrr.com on 2026-11-11]

[DOI: 10.61186/ijrr.24.4.13]

quality. The results indicate that utilizing a large dose optimization grid followed by a small dose calculation grid yields plan quality comparable to using small grids for both processes. Furthermore, photon fluence smoothness levels were found to have no significant impact on these outcomes.

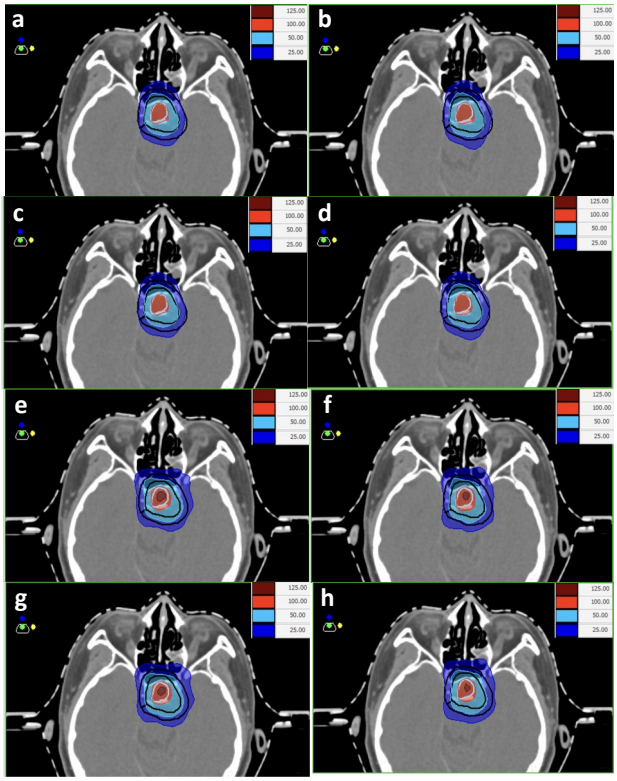


Figure 2. The percent dose distribution of an example SRS case with interplay among photon fluence smoothness, dose optimization grid size, and dose calculation grid size is demonstrated. The left column is a low fluence smoothness, and the right column is a high fluence smoothness. The dose distribution, with an interplay between dose optimization (o) and dose calculation (c), is demonstrated in **(a, b)** o2/c2, **(c, d)** o2/c2, **(e, f)** o3/c2, and **(g, h)** o3/c3 where blue line is target and two layers of black line are the distance of 5 mm and 10 mm from the target.

Funding: This study did not receive research funding.

Conflict of Interest: This study has no conflict of interest.

Ethical consideration: This study protocol was reviewed and approved by the Research Ethics Committee of the Faculty of Medicine, Chiang Mai University. (Study code: RAD-2566-0157)

Author contributions: A.W. - Conceptualization; Data curation; Investigation; Formal analysis, Writing - original draft; Writing - review and editing, W.N. - Conceptualization; Formal analysis; Writing - review and editing; Supervision, A.B. - Formal analysis; Data curation, A.C., B.J. and I.C. - Formal analysis.

REFERENCES

1. Duan Y, Cao H, Wu B, Wu Y, *et al.* (2021) Dosimetric Comparison, Treatment Efficiency Estimation, and Biological Evaluation of Popular Stereotactic Radiosurgery Options in Treating Single Small Brain Metastasis. *Front. Oncol,* ***11****: 716152*.
2. Loftus JP, Shepard M, Liang Y, Yu A, *et al.* (2023) A comparison of single fraction and multi fraction radiosurgery on the gamma knife ICON: A single institution review. *Advance Radiat Oncol,* ***8****: 101161*.
3. Hsu SM, Lai YC, Jeng CC, Tseng CY (2017) Dosimetric comparison of different treatment modalities for stereotactic radiotherapy. *Radiat. Oncol,* ***12****: 155*.
4. Saw CB, Gillette C, Peters CA, Koutcher L (2018) Clinical implementation of radiosurgery using the Helical TomoTherapy unit. *Med. Dosim,* ***43****(3): 284-290*.
5. Watcharawipha A, Chitapanarux I, Jia-Mahasap B (2022) Dosimetric comparison of large field widths in helical tomotherapy for intracranial stereotactic radiosurgery. *Int J Radiat Res,* ***20****(3): 701-707*.
6. Soisson E, Hoban PW, Kammeyer T, Kapatoes JM, *et al.* (2011) A technique for stereotactic radiosurgery treatment planning with helical tomotherapy. *Med. Dosim,* ***36****(1): 46-56*.
7. Greto D, Pallotta S, Masi L, Talamonti C, *et al.* (2017) A dosimetric comparison between CyberKnife and tomotherapy treatment plans for single brain metastasis. *Radiol Med,* ***122****(5): 392-397*.
8. Colombo F, Casentini L, Cavedon C, Scalchi P, *et al.* (2009) Cyberknife radiosurgery for benign meningiomas: short-term results in 199 patients. *Neurosurgery,* ***64****(2): A7-A13*.
9. Xu MC, Khattab MH, Luo G, Sherry AD, *et al.* (2021) Effects of cone versus multi-leaf collimation on dosimetry and neurotoxicity in patients with small arteriovenous malformations treated by stereotactic radiosurgery. *J. Radiosurg. SBRT,* ***7****(4): 287-294*.
10. Murai T, Hattori Y, Sugie C, Iwata H, *et al.* (2017) Comparison of multileaf collimator and conventional circular collimator systems in Cyberknife stereotactic radiotherapy. *J Radiat Res,* ***58****(5): 693-700*.
11. Monk JE, Perks JR, Doughty D, Plowman PN (2003) Comparison of a micro-multileaf collimator with a 5-mm-leaf-width collimator for intracranial stereotactic radiotherapy. *Int J Radiat Oncol Biol Phys,* ***57****(5): 1443-1449*.
12. Snyder Karen C, Liu M, Zhao B, Huang Y, *et al.* (2017) Investigating the dosimetric effects of grid size on dose calculation accuracy using volumetric modulated arc therapy in spine stereotactic radiosurgery. *J Radiosurg SBRT,* ***4****(4): 303-313*.
13. Srivastava SP, Cheng CW, Das IJ (2017) The dosimetric and radiobiological impact of calculation grid size on head and neck IMRT. *Pract Radiat Oncol,* ***7****(3): 209-217*.
14. Park JY, Kim S, Park HJ, Lee JW, *et al.* (2014) Optimal set of grid size and angular increment for practical dose calculation using the dynamic conformal arc technique: a systematic evaluation of the dosimetric effects in lung stereotactic body radiation therapy. *Radiat Oncol,* ***9****(5): 1-12*.
15. Kim KH, Chung JB, Suh TS, Kang SW, *et al.* (2018) Dosimetric and radiobiological comparison in different dose calculation grid sizes between Acuros XB and anisotropic analytical algorithm for prostate VMAT. *PLoS ONE,* ***13****(11): e0207232*.
16. Feuvret L, Noël G, Mazeron JJ, Bey P (2006) Conformity index: a review. *Int J Radiat Oncol Biol Phys,* ***64****(2): 333-342*.
17. Watcharawipha A, Chakrabandhu S, Kongsa A, Tippanya D, Chitapanarux I (2023) Plan quality analysis of stereotactic ablative body radiotherapy treatment planning in liver tumor. *J Appl Clin Med Phys,* ***24****: e13948*.
18. Paddick I (2000) A simple scoring ratio to index the conformity of radiosurgical treatment plans. Technical note. *J. Neurosurg,* ***93****(3): 219-222*.
19. Videtic GM, Hu C, Singh AK, *et al.* (2016) A randomized phase 2 study comparing 2 stereotactic body radiation therapy schedules for medically inoperable patients with stage I peripheral non-small cell lung cancer: nRG Oncology RTOG 0915 (NCCTG N0927). *Int J Radiat Oncol Biol Phys,* ***94****(3): 638*. 10.1016/j.ijrobp.2015.07.2260. [published correction appears in. Timmerman, Robert D [added]] (2015) *Int J Radiat Oncol Biol Phys,* ***93****(4): 757-764*.
20. Desai DD and Cordrey IL (2022) How to estimate R50% for cranial SRS/SRT cases with overlapping 50% isodose volumes: A proposed system. *J Appl Clin Med Phys,* ***23****(7): e13624*.
21. Wagner TH, Bova FJ, Friedman WA, Buatti JM, *et al.* (2003) A simple and reliable index for scoring rival stereotactic radiosurgery plans. *Int J Radiat Oncol Biol Phys,* ***57****(4): 1141-1149*.
22. Vuthiwong W, Watcharawipha A, Jia- Mahasap B, Nobnop W, Chitapanarux I (2022) Clinical and radiological response of aggressive dural arteriovenous fistula after combined glue

[Downloaded from mail.ijrr.com on 2026-11-11]

[DOI: 10.61186/ijrr.24.4.13]

embolization and hypofractionated helical TomoTherapy. *J Radiotherapy in Practice, **21**(4): 513-518*.
23. Kongsa A, Chitapanarux I, Watcharawipha A, Huntrakul L, *et al.* (2023) Improvement of matching fields using coplanar field border method in postmastectomy radiotherapy. *Journal of Radiotherapy in Practice, **22**(e8): 1-8*.
24. Ayman N, Abdelaal A, Amer HH, Mohammed HS (2025) Impact of slice thickness and grid size on dose calculation in intensity modulated and volumetric-modulated are radiotherapy in head and neck cancer. *Int J Radiat Res, **23**(2): 263-270*.
25. Tongta S, Watcharawipha A, Nobnop W, Wanwilairat S, Tongsuk W (2025) Evaluation of various resolutions for optimization and dose calculation in VOLO™ Ultra of the TomoTherapy treatment planning system. *Biomed. Sci Clin Med, **64**(2): 1-13*.
26. Karen SC, Liu M, Zhao B, Huang Y, *et al.* (2017) Investigating the dosimetric effects of grid size on dose calculation accuracy using volumetric modulated arc therapy in spine stereotactic radiosurgery. *J Radiosurg SBRT, **4**(4): 303-313*.
27. Shimizu H, Sasaki K, Tanaka H, Aoyama T, *et al.* (2020) Dosimetric effects of dose calculation grid size on the epidural space dose. *Med Dosim, **45**(4): 327-333*.

[Downloaded from mail.ijrr.com on 2026-11-11]

[DOI: 10.61186/ijrr.24.4.13]

[DOI: 10.61186/ijrr.24.4.13] [Downloaded from mail.ijrr.com on 2026-11-11]